Supporting Information

Synergistic Effect of Fluorination and Regio-regularity on Long-term Thermal Stability of Polymer Solar Cells

Zidong Li, Tong Zhang, Yue Xin, Xiaoli Zhao, Dalei Yang, Fan Wu and Xiaoniu Yang**

Z. Li, T. Zhang, Y. Xin, Dr. X. Zhao, D. Yang, F. Wu, Prof. X. Yang
State Key Laboratory of Polymer Physics and Chemistry, Changchun Institute of Applied Chemistry, Chinese Academy of Sciences, 5625 Renmin Street, Changchun, 130022, P.R. China
Z. Li, T. Zhang, Y. Xin, Dr. X. Zhao, D. Yang, F. Wu, Prof. X. Yang
Polymer Composites Engineering Laboratory, Changchun Institute of Applied Chemistry, Chinese Academy of Sciences, Renmin Str. 5625, Changchun 130022, P.R. China
E-mail: xnyang@ciac.ac.cn, zhaoxiaoli@ciac.ac.cn
Z. Li, T. Zhang, Y. Xin, D. Yang, F. Wu
University of Chinese Academy of Sciences, Beijing 100049, P.R. China

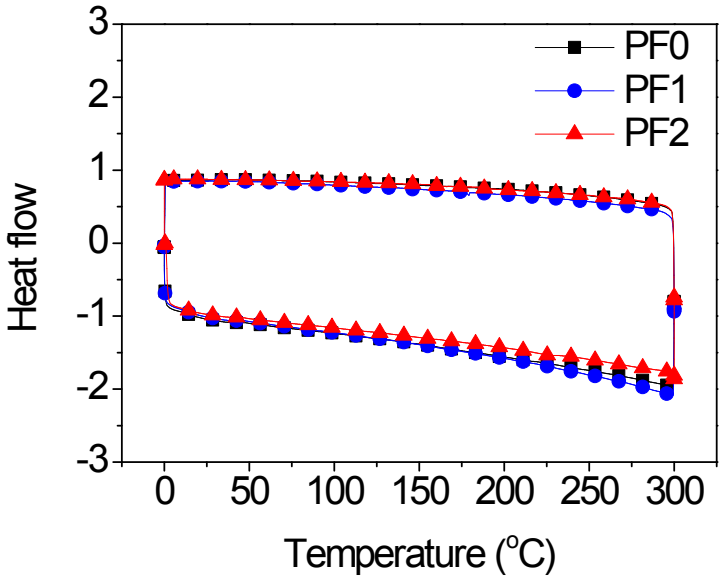

Figure S1 Differential scanning calorimetry (DSC) curves of PF0, PF1 and PF2.

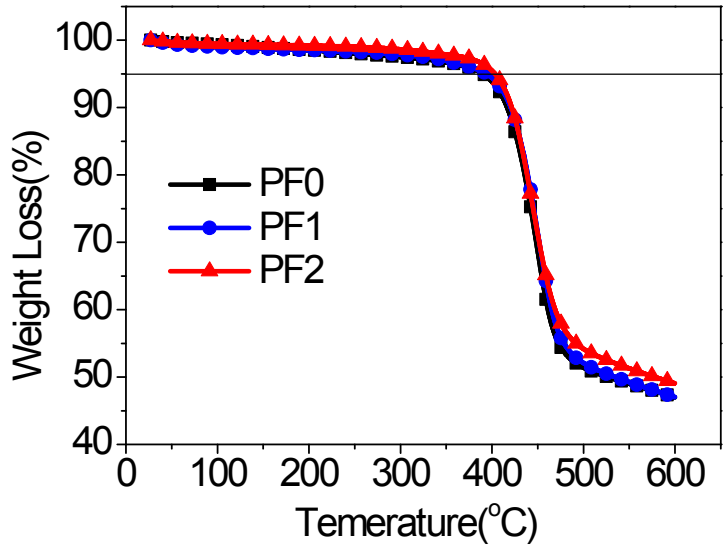

Figure S2 Thermogravimetric analysis (TGA) curves of PF0, PF1 and PF2.

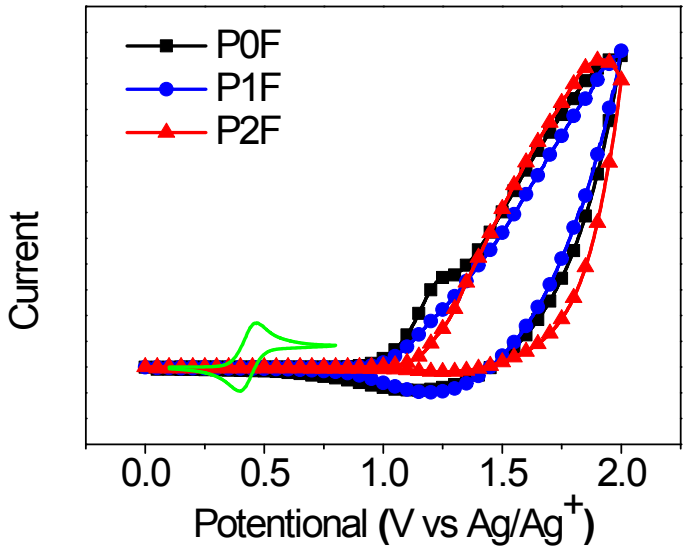

Figure S3 Cyclic voltammogram of PF0, PF1 and PF2 films casted from chlorobenzene *vs.* the SCE in 0.1 M Bu_4NPF_6/acetonitrile solution.

Table S1 Photovoltaic parameters of devices based on PF0, PF1 and PF2.

Polymers	D/A ratio	V_{oc} (V)	J_{sc} (mA cm^{-2})	FF (%)	PCE(%) Best/Ave[a]	Film Thickness (nm)
PF0	1/2	0.74	10.66	60.67	4.79/4.61	94
	1/1.5	0.74	11.25	59.65	4.96/4.60	95
	1/1 [b]	0.70	9.46	49.21	3.26/3.02	96
	1/1	0.74	11.76	65.46	5.70/5.62	97
PF1	1/2	0.78	11.21	60.48	5.29/4.95	105
	1/1.5	0.80	11.03	60.25	5.32/5.04	110
	1/1 [b]	0.74	11.05	54.65	4.47/4.06	100
	1/1	0.80	11.85	66.23	6.29/6.13	98
PF2	1/2	0.82	10.51	54.27	4.67 /4.41	114
	1/1.5	0.84	10.58	60.65	5.39 /5.24	97
	1/1 [b]	0.81	9.89	56.85	4.56/4.38	106
	1/1	0.86	11.67	65.25	6.55/6.45	101

[a] Average PCE obtained on 8 devices.

[b] Without thermal annealing treatment.

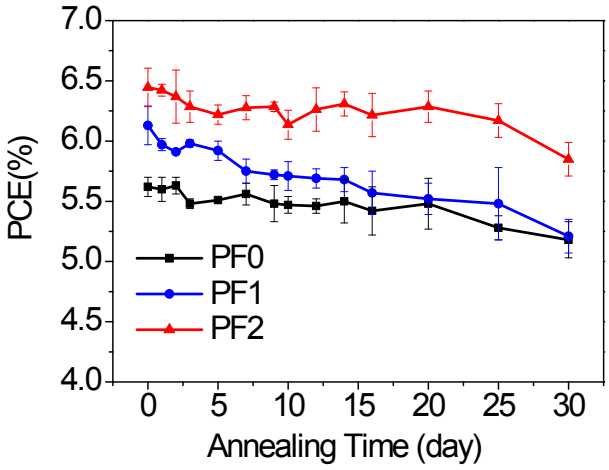

Figure S4 Annealing time-dependent PCE of PF0, PF1 and PF2 devices as a function of time at 100 °C.

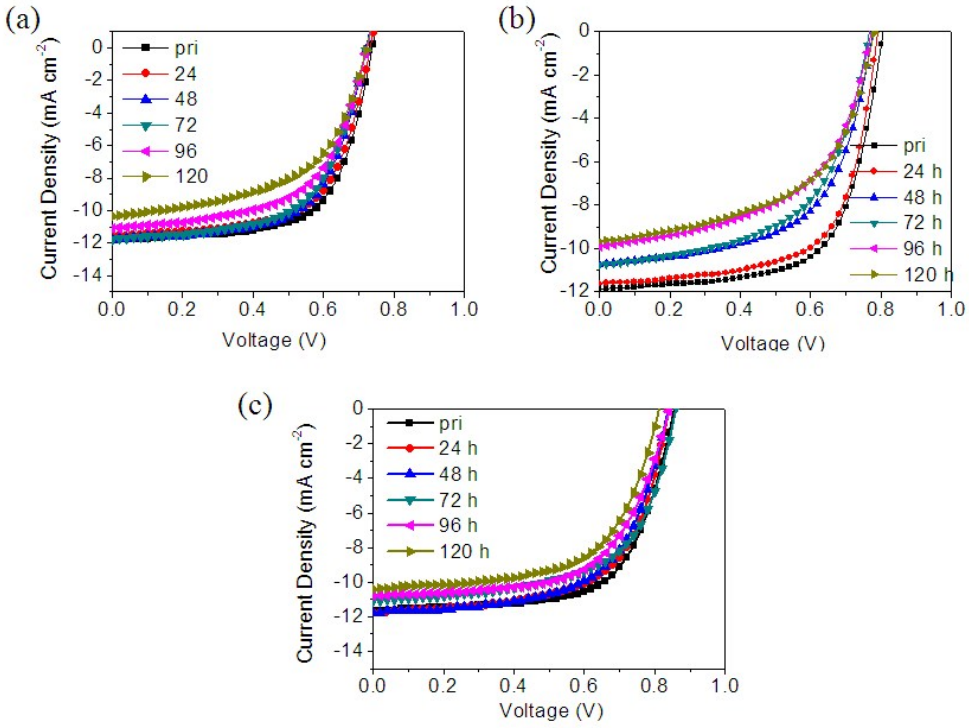

Figure S5 *J-V* characteristic curves of PF0, PF1 and PF2 devices as a function of annealing time at 130°C.

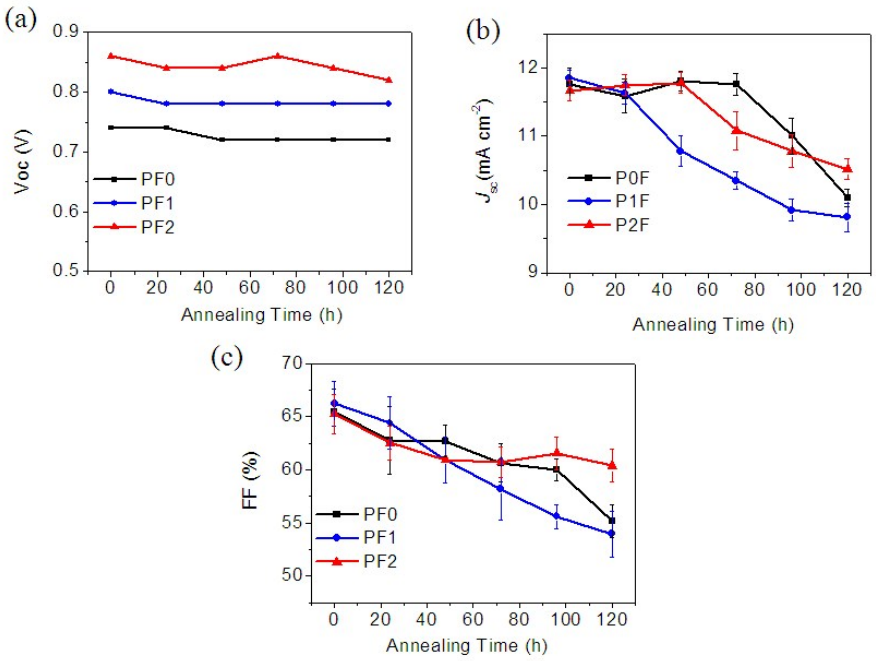

Figure S6 Variations of (a) V_{oc}, (b) J_{sc} and (c) FF of PF0, PF1 and PF2 devices as a function of annealing time at 130 °C.

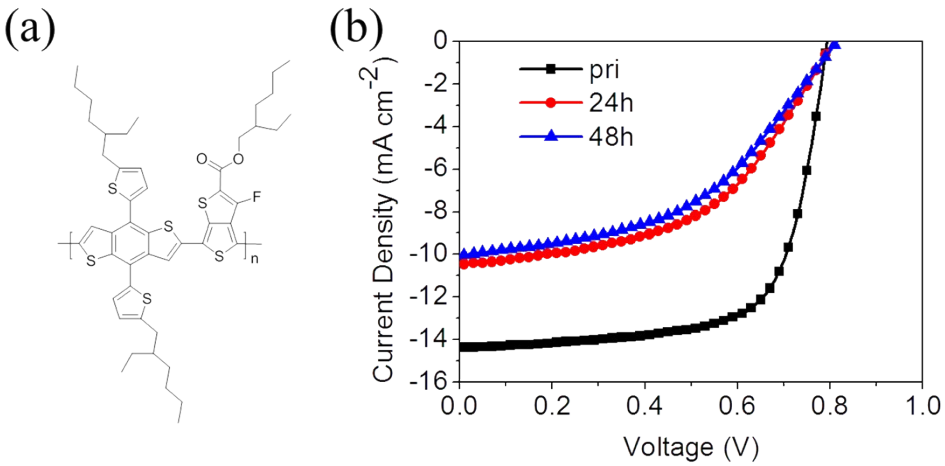

Figure S7 (a) The structure of PTB7-Th, (a) *J-V* characteristic curves of PTB7-Th device annealed at 130°C, with conventional structure of ITO/PEDOT: PSS/polymer: PCBM/Ca/Al.

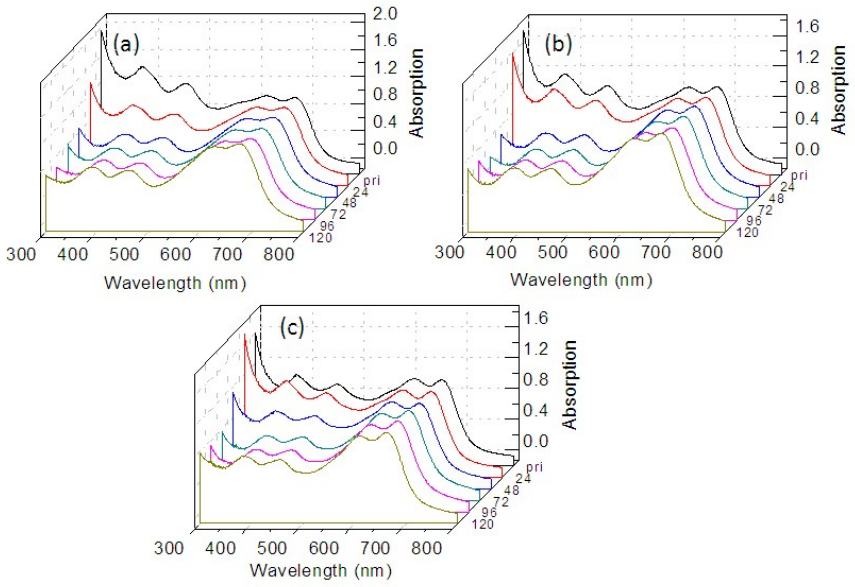

Figure S8 UV-vis absorption spectra of PF0 (a), PF1 (b) and PF2 (c) blends after thermal annealing for different times at 130°C.

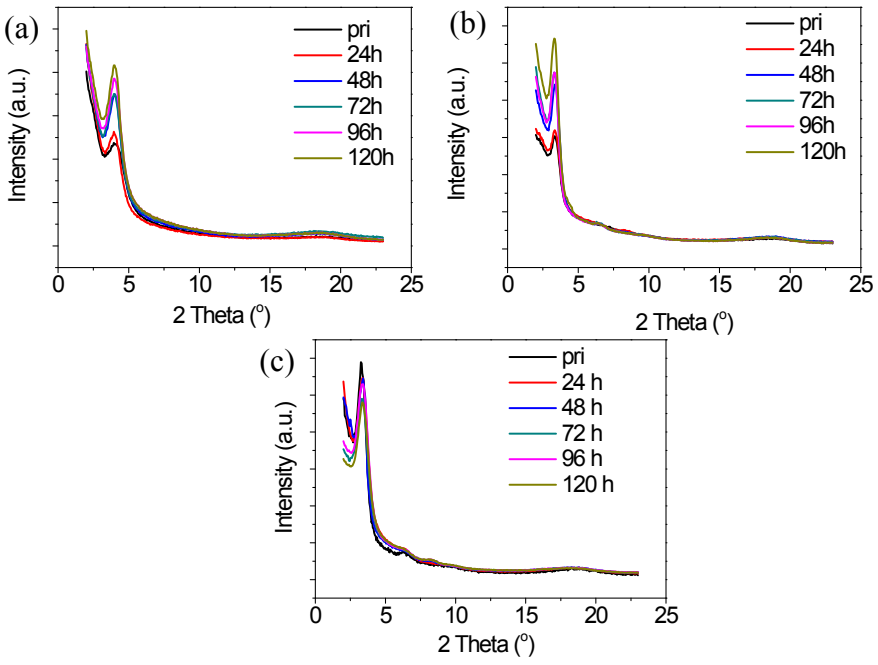

Figure S9 The out-of plane XRD spectra of PF0 (a), PF1 (b) and PF2 (c) blends after thermal annealing for different times at 130°C.

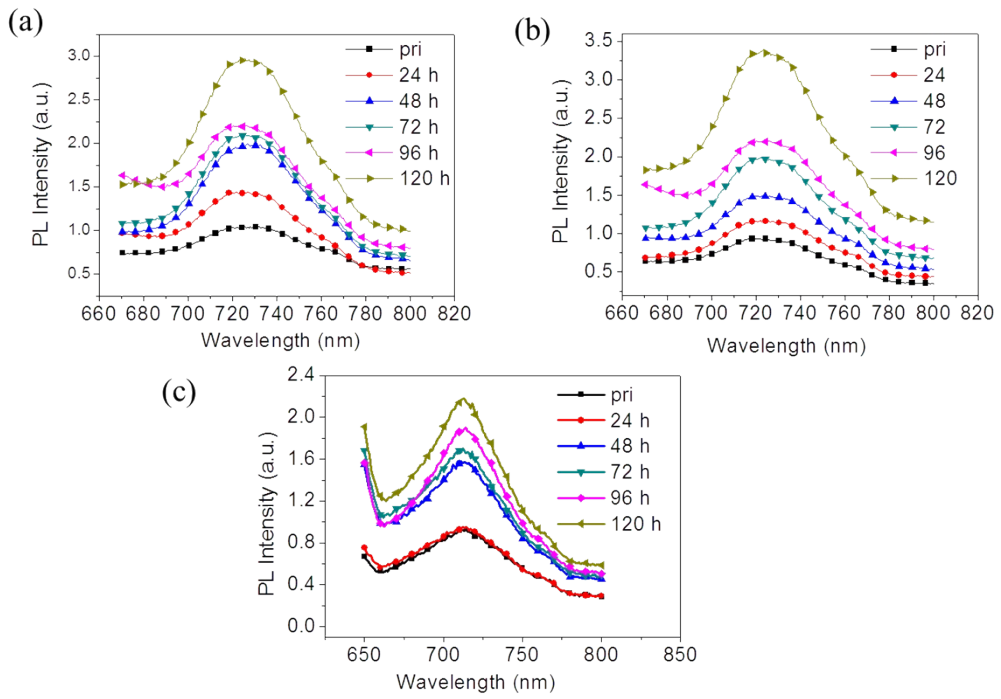

Figure S10 The photoluminescence (PL) spectra of PF0 (a), PF1 (b) and PF2 (c) blends after thermal annealing for different times at 130 °C.

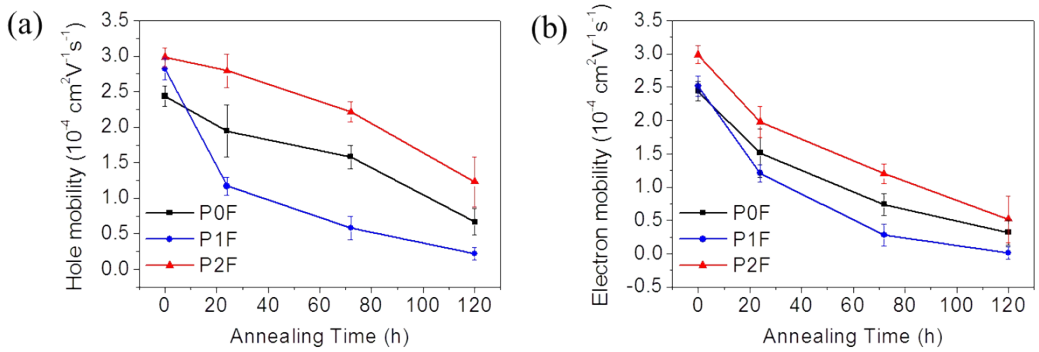

Figure S11 Electron mobility (a) and hole mobility (b) of PF0, PF1 and PF2 blends as a function of annealing time at 130 °C measured by the space-charge-limited current (SCLC) method with the device structure of ITO/TIPD/Polymer: PCBM/Ca/Al (for electron mobility) and ITO/ PEDOT: PSS /Polymer: PCBM/Au /Al (for hole mobility).

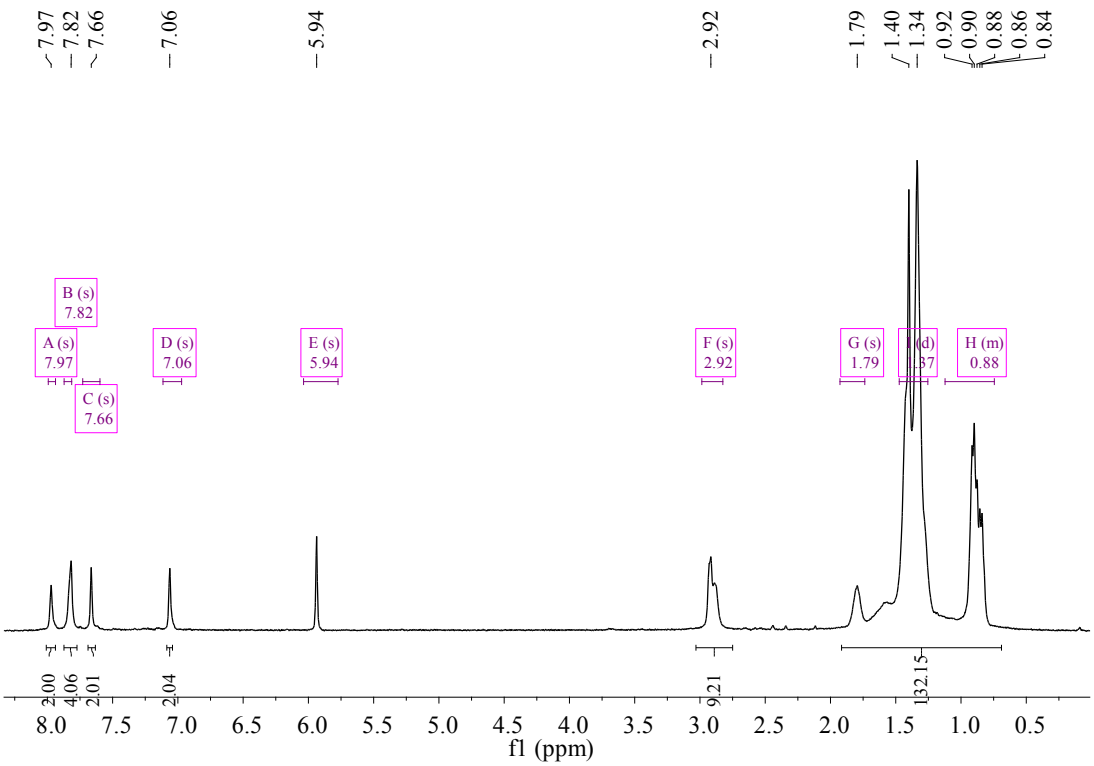

Figure S12 ^{1}H-NMR spectrum of PF0 polymer.

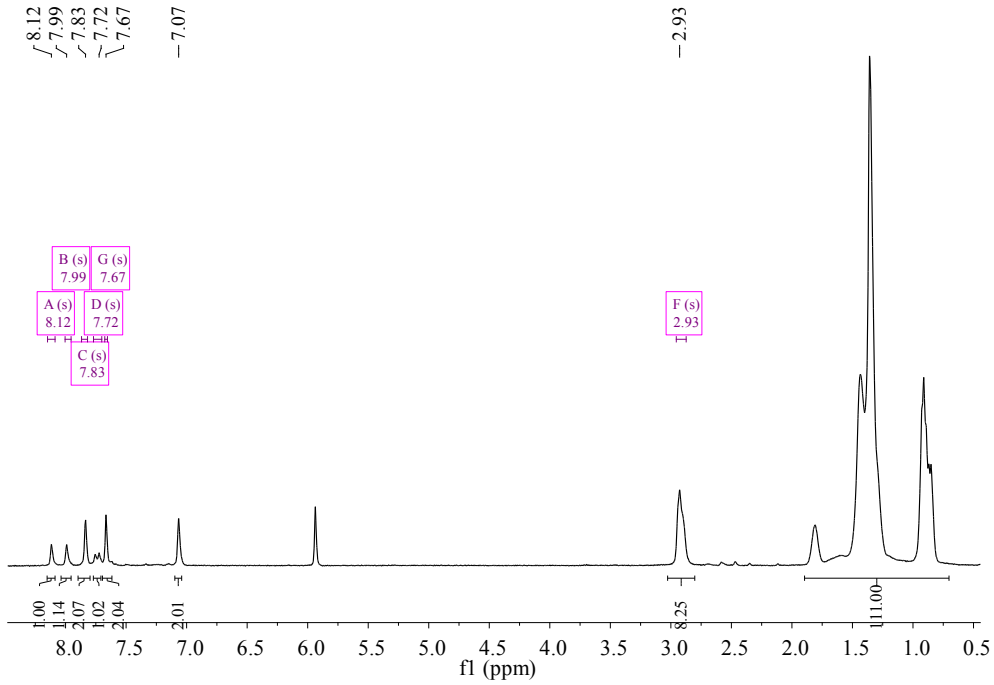

Figure S13 ^{1}H-NMR spectrum of PF1 polymer.

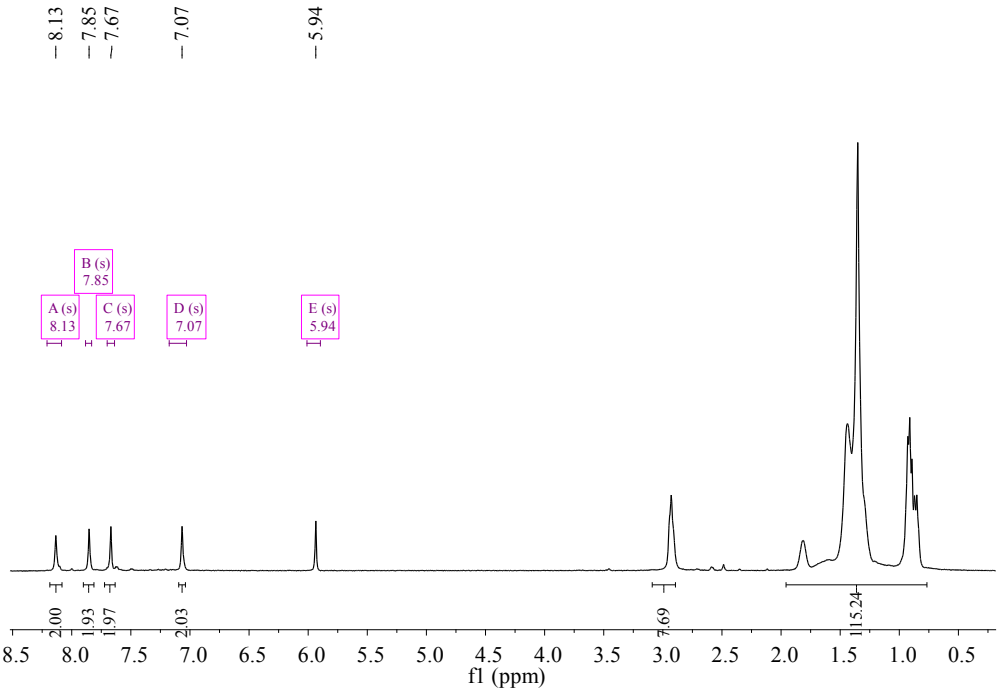

Figure S14 ^{1}H-NMR spectrum of PF2 polymer.